Pakistan Veterinary Journal

ISSN: 0253-8318 (PRINT), 2074-7764 (ONLINE)
DOI: 10.29261/pakvetj/2026.036

RESEARCH ARTICLE

# Inhibition of Porcine Reproductive and Respiratory Syndrome Virus Infection by *Macleaya cordata* Extract Targeting EGFR

Yongneng Li[†1,2], Jiaxing Sun[†2], Shanshan Qi[2], Xinxian Wang[2], Wenjuan Su[2], Qian Li[2], Yongmei Li[2], Junlong Bi[2], Gefen Yin[2*] and ZhenLei Zhou[1*]

[1]College of Animal Veterinary Medicine, Nanjing Agricultural University, Nanjing, Jiangsu, China; [2]College of Animal Veterinary Medicine, Yunnan Agricultural University, Kunming, Yunnan, China
[†]Yongneng Li and Jiaxing Sun have equal contributions
*Corresponding author: Yingefen0616@163.com (FGY); zhouzl@njau.edu.cn (ZLZ)

ARTICLE HISTORY (25-1201)

Received: December 06, 2025
Revised: February 22, 2026
Accepted: February 24, 2026
Published online: February 25, 2026

**Key words:**
Antiviral activity
EGFR
Infection
*Macleaya cordata* extract
Porcine reproductive and Respiratory syndrome virus (PRRSV)

**ABSTRACT**

Porcine reproductive and respiratory syndrome (PRRS), an important infectious disease of swine caused by porcine reproductive and respiratory syndrome virus (PRRSV), is one of the most important infectious diseases threatening the pig industry. *Macleaya cordata* extract (MCE), a traditional Chinese medicine, is known for its antibacterial, anti-inflammatory, and antioxidant properties. Its anti-PRRSV activity and underlying mechanism remain unclear. In the present study, MCE was found to have anti-PRRSV activity and a favorable drug safety profile. MCE inhibited PRRSV proliferation dose-dependent manner, suppressing PRRSV adsorption and internalization. Furthermore, network pharmacology and molecular docking analysis were utilized to predict that EGFR may be a potential target of MCE. Meanwhile, the results showed that MCE inhibits PRRSV proliferation by suppressing the expression of EGFR and phosphorylation. The BLI results showed that the binding of MCE to EGFR was concentration-dependent, further confirming that MCE exerts its antiviral effect by targeting EGFR. In conclusion, the MCE exhibits a potent antiviral effect against PRRSV, providing evidence for the antiviral mechanism of MCE.

**To Cite This Article:** Li Y, Sun J, Qi S, Wang X, Su W, Li Q, Li Y, Bi J, Yin G and Zhou Z, 2026. Inhibition of porcine reproductive and respiratory syndrome virus infection by macleaya *cordata* extract targeting EGFR. Pak Vet J, 46(2): 473-484. http://dx.doi.org/10.29261/pakvetj/2026.036

## INTRODUCTION

Porcine reproductive and respiratory syndrome (PRRS) is a highly contagious viral disease that mainly causes reproductive disorders in sows, high morbidity and mortality in newborn piglets, and respiratory diseases in pigs of all ages. This disease has caused significant economic losses to the pig industry worldwide (Guo *et al.*, 2018). The pathogen is the porcine reproductive and respiratory syndrome virus (PRRSV), a member of the genus *Arterivirus* within the family *Arteriviridae* (Lunney *et al.*, 2016). PRRSV has two genotypes: PRRSV-1 (European type, Lelystad) and PRRSV-2 (American type, VR-2332), which share approximately 60% nucleotide homology.

PRRS was first reported in the United States in 1987 (Keffaber, 1989) and has since been gradually reported worldwide (Wensvoort *et al.*, 1991; Collins *et al.*, 1992; Wensvoort *et al.*, 1992; Kuwahara *et al.*, 1994; Albina, 1997; Forsberg *et al.*, 2002; Lin *et al.*, 2020). PRRS was first reported in China in 1995 (Guo *et al*., 1996; Yang *et al*., 1997), with the PRRSV-2 strain (CH-1a) being the predominant strain. Highly pathogenic PRRSV (HP-PRRSV) triggered a massive outbreak of atypical PRRS in China during the summer of 2006, resulting in significant damage to the pig industry (Tian *et al.*, 2007). In 2008, the NADC30 strain, which has three non-contiguous amino acid deletions in the Nsp2 coding region (amino acids 322-432, 483, and 504-522), totaling 131 amino acids, was isolated in the United States (Wang *et al.*, 2018). In 2013, the NADC30 strain entered China and recombined with the local HP-PRRSV strain, producing an NADC30-like strain characterized by low fever and stillbirths, which gradually became one of the most significant epidemics in China's large-scale main farms ( Tian *et al*., 2007; Li *et al.*, 2016; Guo *et al*., 2018). Studies have shown that the emergence and mutation of NADC30-like strains are responsible for the resurgence of a widespread PRRS epidemic (Zhou *et al.*, 2015; Li *et al*., 2016). In 2018, NADC34-like strains were identified in Liaoning, China, and subsequently became the dominant strains (Zhang *et al.*, 2018; Xu *et al.*, 2022). Recent studies have identified the NSP5-NSP9

region, especially the S2/S3 junction, as a recombination hotspot between NADC30-like and HP-PRRSV strains through phylogenetic and recombination analyses (Chang *et al.*, 2024; Jiao *et al.*, 2024). The emergence of NADC34-like strains has been reported in several provinces in China, indicating a gradual epidemic of NADC34-like strains in China (Zhao *et al.*, 2022).

Vaccines are one of the most effective means of clinical control of PRRS and modified live and inactivated vaccines have been marketed. Additionally, DNA vaccines, subunit vaccines, and vector vaccines have also been extensively studied (Chen *et al.*, 2022). However, existing vaccines primarily protect against homologous strains, with limited cross-protection against heterologous strains (Chen *et al*., 2022). PRRS infections are frequently followed by secondary infections from opportunistic pathogens. Farms typically resort to drugs like clindamycin or aspirin for symptom relief due to inadequate treatment options. However, improper antibiotic use on some farms contributes to pathogen resistance, drug residues, and environmental pollution, complicating disease management (Manyi-Loh *et al.*, 2018; VanderBurgt *et al.*, 2023).

Herbal medicines are generally characterized by various biological activities (Chen and Yu, 1999). Herbal medicines employ various strategies to exhibit antiviral effects, including direct virus elimination, virus eradication through active compounds, hindering virus attachment and entry, and suppressing virus replication, thereby eliminating pathogens from the body (Holmes *et al.*, 2019). *Macleaya cordata*, a traditional Chinese medicinal herb, is a perennial plant belonging to the genus *Macleaya*, within the family *Papaveraceae.* The main constituents contain various active alkaloids, such as *haematogenine* and *leucoerythrine* (Kosina *et al.*, 2010; Shi *et al.*, 2015), which have antibacterial, anti-inflammatory, and antioxidant effects (Lin *et al.*, 2018). In 2023, researchers have reported that a small molecule compound, *haematogenine*, extracted from traditional Chinese medicine has antiviral activity against PRRSV, and that *haematogenine* with *albizia rhododendron* was able to increase the antiviral activity against PRRSV (Ke *et al.*, 2023).

This study investigated the anti-PRRSV infection activity of *Macleaya cordata* extract (MCE) and its mechanism, to provide experimental evidence for its potential application.

## MATERIALS AND METHODS

**Drugs and Reagents:** *Macleaya cordata* extract (MCE) (SS2302, 60%HPLC, purity: 99%) was purchased from Hubei Shishun Biotechnology Co. Ltd. *Tilmicosin* (HY-B0905A) was purchased from MedChemExpress.

**Viruses and Cells:** The strain used in the experiment was the PRRSV YN-1 strain (GenBank no. KJ747052.1), which was isolated and preserved in our laboratory and belongs to PRRSV genotype II. Marc-145 cells (susceptible cells) and PAM cells (host cells) were cultured in Dulbecco's Modified Eagle's Medium (DMEM) supplemented with 10% fetal bovine serum (FBS, Gibco, Franklin Lakes, NJ, USA). Additionally, the culture medium for PAM cells was supplemented with 5μL/mL mycoplasma inhibitor and 3 μg/mL puromycin.

**Cell Viability Assay:** Cells were seeded on a 96-well plate at a density of $1.2\times10^4$ cells per well. When the cells in each well reached 80-90% confluence, different concentrations of MCE (ranging from 100 to 0.19mg/mL, diluted at a 2-fold ratio) were added. The viability of cells treated with different concentrations of MCE for 12, 24, 36, 48, 60, 72, and 84 hours was evaluated using the CCK-8 assay. Data was processed, and the $CC_{50}$, $EC_{50}$, and selection index (SI; the ratio of $CC_{50}$ to $EC_{50}$) were calculated using the statistical software GraphPad Prism 9.

**The Cell Treatments of MCE:** MCE was diluted to 0.19 - 6.25mg/mL according to the $CC_{50}$ (2-fold dilution, a total of 6 concentrations), and the tilmicosin positive control group (10mM) was used as positive control.

The *in vitro* resistance of MCE to PRRSV was evaluated by three treatment methods: pre-incubation, post-incubation, and co-incubation. Preventive effect (pre-incubation): Cells were incubated with different concentrations of MCE at 37℃ for 2 hours, and then 0.1 MOI PRRSV was inoculated for 2 hours. Therapeutic effect (post-incubation): A MOI of 0.1 PRRSV was inoculated onto the cells for 2 hours, followed by incubation with different concentrations of MCE for 2 hours. Direct action therapy (co-incubation) involved directly mixing PRRSV with different concentrations of MCE, incubating at 37°C for 2 hours, and then inoculating onto cells for 2 hours.

**RNA Isolation and Quantitative Real-time PCR:** Total RNA was extracted using RNAiso Plus (Takara; 9091), and cDNA was synthesized by reverse transcription according to the methods of Bi *et al*. (2018) and Liu *et al*. (2019). The relative mRNA expression levels of EGFR, ESR1, and TP53 were obtained by quantitative real-time polymerase chain reaction (qRT-PCR), normalized to the expression level of GAPDH as a reference, and calculated using the $2^{-\Delta\Delta Ct}$ method. The absolute mRNA level of PRRSV ORF7 was calculated using a standard curve, in which the PRRSV ORF7 standard plasmid was constructed in our laboratory (Wang *et al.*, 2023), and this plasmid was diluted 10-fold to generate the standard curve. The qRT-PCR experiment was performed according to the previously established system in our laboratory (Wang *et al*., 2023).

The transcriptional levels of different genes were detected using specific primers (Table 1).

**Table 1:** Primer Information

| Primer Name | Primer Sequence (5' to 3') | Primer Length (nt) | Tm℃ |
|---|---|---|---|
| ORF7-F | AATGGCCAGCCAGTCAATCA | 20 | 57.5 |
| ORF7-R | TCATGCTGAGGGTGATGCTG | 20 | |
| GAPDH-F | TGGAAAAACCTGCCAAGTACG | 20 | 58 |
| GAPDH-R | ATGAGGTCCACCACCCTGTT | 20 | |
| EGFR-F | TGCCCCAGGTCATGAACATC | 20 | 53 |
| EGFR-R | ATCTTAGGCCCGTTCCTTGC | 20 | |
| ESR1-F | ACAGGCCAAATTCAGATAATCG | 22 | 57 |
| ESR1-R | CTCTTCCTCCTGTTCTTATCAA | 22 | |
| TP53-F | GTCTGGGCTTCCTGCATTCT | 20 | 59 |
| TP53-R | GGGGTGTGGAATCAACCCA | 19 | |

**Indirect Immunofluorescence Assay:** The cultured cells were washed three times with PBS, then fixed with pre-cooled methanol and washed again with PBS. The cells were blocked with 5% bovine serum albumin at 37°C for 2

hours, then incubated with primary and secondary antibodies for 12 hours each, followed by treatment with 4′,6-diamidino-2-phenylindole (DAPI, Beyotime; C1005) for 10 minutes. Fluorescence images were captured using an Olympus FV10 laser scanning confocal microscope (Olympus, Tokyo, Japan).

**Western Blotting:** Samples were lysed using RIPA Lysis Buffer (Beyotime, P0013B), and the lysates were collected for Western blot analysis as described previously (Bi *et al*., 2018). Protein samples were separated by sodium dodecyl sulfate-polyacrylamide gel electrophoresis and transferred to 0.22-μm PVDF membranes (Millipore, Bedford, MA, USA) using the wet transfer method. The membranes were blocked with 5% (w/v) skim milk for 2 hours at 4°C and then incubated overnight at 4°C with primary antibodies. The secondary antibodies used were HRP-conjugated anti-rabbit (Proteintech, Cat: RGAR001) and HRP-conjugated anti-mouse (Proteintech, Cat: RGAM001). Images were captured using chemiluminescent ECL Plus substrate (Pierce, Rockford, IL) and analyzed with ImageJ software (version 1.8.0 for Windows).

**Median tissue culture infective dose ($TCID_{50}$) Assay:** To determine the effect of MCE on the titer of PRRSV. Based on previous results, the co-incubation treatment was selected with the most significant inhibitory effect. Cells were seeded in 96-well plates at a cell density of $1.2 \times 10^5$ cells per well. When the cell density reached 80-90%, 100 μL of virus, serially diluted tenfold, was inoculated. The cytopathic effect (CPE) of cells at different dilution ratios was observed every 12 hours, and the cell lesion conditions were recorded. The virus titer was calculated using the Reed and Muench method.

**Network Pharmacology Analysis:** The active chemical constituents of the MCE were searched for using the HERB online database (http://herb.ac.cn/) and verified using the SwissADME online website (http://www.swissadme.ch/index.php) (Bi *et al*., 2018). The active constituents-related targets were gathered from TCMSP (http://lsp.nwu.edu.cn/tcmsp.php), SwissTargetPrediction (http://www.swisstargetpredECtion.ch/), SEA Search Server (http://www.bkslab.org), and Pubchem databases (https://pubchem.ncbi.nlm.nih.gov). PRRSV-related targets were collected via the Comparative ToxECogenomECs Database (http://www.ctdbase.org). The overlap between the disease and drug component targets was evaluated using Venny 2.1.0. The STRING 11.5 database (https://string-db.org) was used to construct a PPI network of shared targets between drug components and diseases. Utilizing the Cytoscape software, the network topology parameters of targets were analyzed, including degree, betweenness, and closeness, to uncover important nodes in the network through maximizing group mining of network modules.

*2.10 Homology Modeling and Molecular Docking Analysis*

A three-dimensional (3D) model of the EGFR was constructed using the SwissModel web server (https://swissmodel.expasy.org/). Subsequently, the 3D structures were energy-minimized using Swiss-PDB Viewer 4.1.0. The quality and accuracy of the improved model were assessed using the SAVES server (https://saves.mbi.ucla.edu) tool, and Ramachandran plots of EGFR were generated using the PROCHECK function. The structural formulas of the seven active compounds from the MCE were downloaded from the public chemical database PubChem (https://pubchem.ncbi.nlm.nih.gov), and the compound formats were converted to PDB format using OpenBabel 3.0.1 software. EGFR structures that had been energy-minimized were processed using the Protein Preparation Wizard function of the Maestro 12.9 software in the Schrödinger Suite. Compound structures were processed using the LigPrep function, during which they were predicted using the online server CavityPlus (http://www.pkumdl.cn/cavityplus/) to predict the activity pockets of the docked EGFR molecules, followed by flexible docking of the EGFR proteins and seven small molecule compounds using the Glide module of the Maestro 12.9 software to analyze the binding pattern and score (GlideScore). The protein-small molecule interactions were then visualized in the Maestro interface.

**Knockdown of EGFR by Silencing RNA:** The two small interference RNAs (siRNAs) targeting the swine EGFR were synthesized (Table 2).

**Table 2:** Sequences of siRNAs used in this study

| Primer Name | Primer Sequence (5' to 3') | Target Gene |
|---|---|---|
| si-EGFR1-F | CGGAAUAGGUAUUGGUGAAUU | EGFR |
| si-EGFR1-R | AAUUCACCAAUACCUAUUCCG | EGFR |
| si-EGFR2-F | GGAGAUAAGCGAUGGAGAUGU | EGFR |
| si-EGFR2-R | ACAUCUCCAUCGCUUAUCUCC | EGFR |

Cells grown to approximately 80-90% confluence in 6-well plates were transfected with siRNA-EGFR (50 nM/well) or siRNA-NC (50 nM/well), respectively, using Lipofectamine™ 3000 (Invitrogen; L3000-05) according to the manufacturer's instructions. Twelve hours post-transfection (hpi), the cells were washed three times with PBS and infected with the PRRSV strain YN-1 at a 0.1 MOI. At 24 hpi, samples were subjected to PRRSV RNA and protein detection by qRT-PCR and Western blotting, respectively.

**Bio-Layer Interferometry Assay:** Bio-Layer Interferometry (BLI) is used to evaluate interactions between different molecules. The intermolecular interactions between EGFR and MCE were detected using BLI technology with the ForteBio Octet Red system (ForteBio, Inc., Menlo Park, USA). Buffer composition: PBS (pH 7.4) + 0.01% Tween-20. Biotinylation of EGFR extracellular domain proteins expressed in *Escherichia coli* was performed using Biotin NHS (MedChemExpress; HY-D0802). The reaction mixture was desalted using a Zeba Spin desalting column (Thermo Fisher Scientific; 89882). The EGFR protein was attached to the SSA biosensor (Cat: 18-5056; ForteBio) and then immersed in wells with different MCE concentrations (100, 200, and 400μM). The control group used sensors without MCE-loaded proteins to correct baseline drift. The control reaction was carried out in solutions with different ligand concentrations, but without the loaded protein. The association and dissociation responses were processed using Octet Data Analysis Software (Version 7.0; ForteBio). The

interferometric measurement data were fitted using the Langmuir 1:1 binding model. The chart was created using GraphPad Prism 9.0 (GraphPad Software, Inc.).

**Statistical analysis:** All data are expressed as mean ± standard deviation (n=3). All statistical analyses were conducted using GraphPad Prism 8 software. When comparing two groups, the Student's t-test was used for statistical analysis. When more than two groups were compared, one-way analysis of variance (ANOVA) was used for statistical analysis. The significance levels are denoted as * P<0.05, ** P<0.01, and *** P<0.001.

## RESULTS

**MCE exhibits anti-PRRSV activity:** To determine the concentration of MCE used in the following experiments, we employed the CCK-8 method to evaluate the cytotoxicity of MCE on Marc-145 and PAM cells. The $CC_{50}$ of MCE on Marc-145 and PAM cells was 12.45 and 17.01mg/mL, respectively. There was no significant cytotoxicity of MCE on Marc-145 and PAM cells at concentrations equal to or less than 6.25mg/mL (Fig. 1A).

*Tilmicosin* has been proven to have an inhibitory effect on PRRSV infection and can be used as a positive control. *Tilmicosin* had a $CC_{50}$ of 386.3 mg/mL against Marc-145 cells and 410.3mg/mL against PAM cells. At concentrations of 100 mg/mL or lower, *tilmicosin* had no significant cytotoxic effects on Marc-145 and PAM cells (Fig. 1B). In the pre-incubation assay, the $EC_{50}$ of MCE against PRRSV was 0.79 mg/mL in Marc-145 cells and 1.13 mg/mL in PAM cells; the $EC_{50}$ of *tilmicosin* was 31.25 mg/mL in Marc-145 cells and 32.23mg/mL in PAM cells (Fig. 1C); In the post-incubation assay, the $EC_{50}$ of MCE against PRRSV was 0.93 mg/mL in Marc-145 cells and 1.24mg/mL in PAM cells; the $EC_{50}$ of *tilmicosin* was 47.54mg/mL in Marc-145 cells and 60.6 mg/mL in PAM cells (Fig. 1D); and in the co-incubation assay, the $EC_{50}$ of MCE against PRRSV was 0.57 mg/mL in Marc-145 cells and 0.56 mg/mL in PAM cells; the $EC_{50}$ of *tilmicosin* was 56.16 mg/mL in Marc-145 cells and 69.18 mg/mL in PAM cells (Fig. 1E). The selection index (SI) is a crucial indicator for evaluating the safety of a drug, calculated by comparing the $CC_{50}$ and $EC_{50}$ values of the drug. In the co-incubation assay, the SI index of MCE was the highest, at 21.84 and 30.38, respectively, in Marc-145 cells and PAM cells.

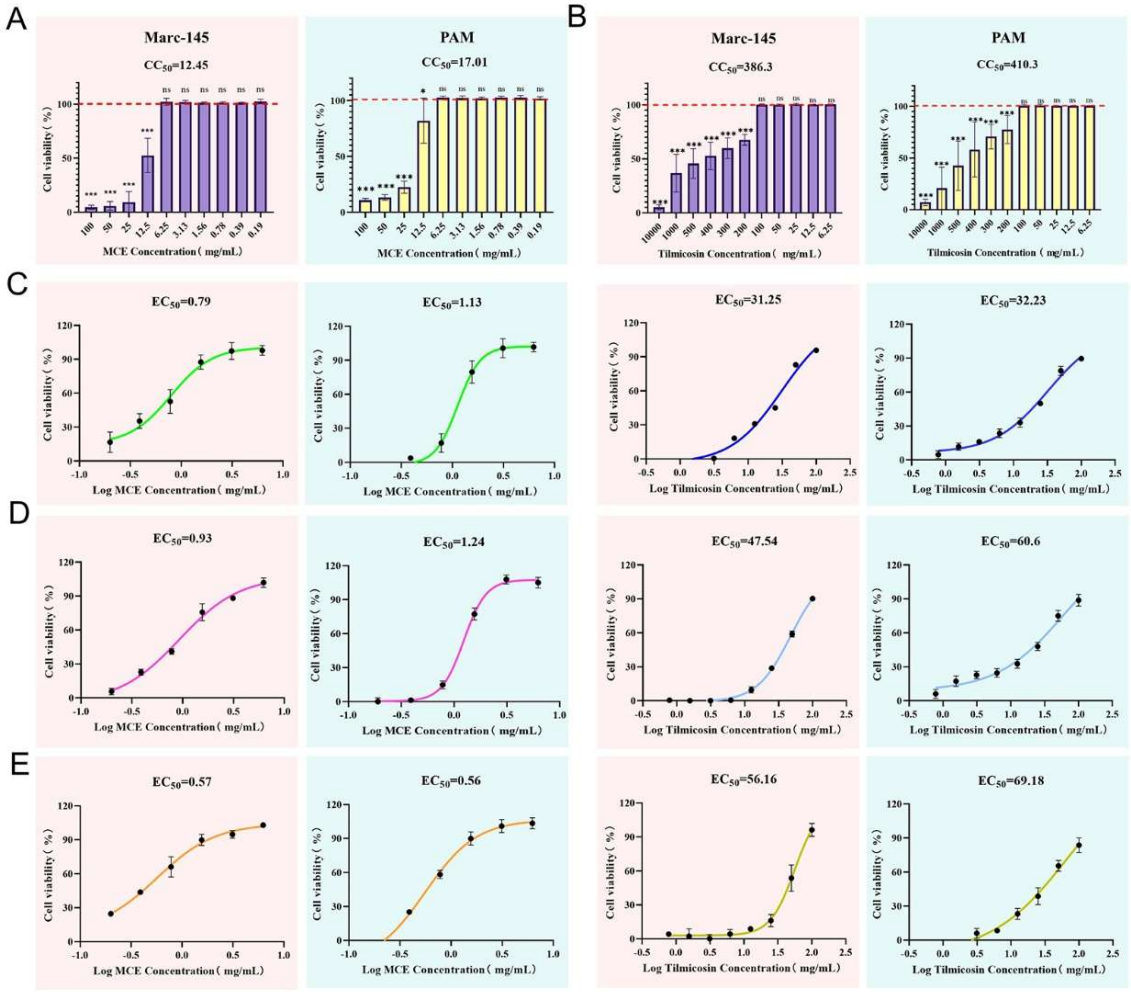


**Fig. 1:** The toxicity of MCE to Marc-145/PAM cells and its inhibitory effect on PRRSV. (A) The cells were incubated with MCE at various concentrations (0.19-100 mg/mL) for 72 hours. Determination of median cytotoxic concentration ($CC_{50}$) of MCE using the CCK-8 method. (B) The $CC_{50}$ determination of Tilmicosin. (C) The Median effective concentration ($EC_{50}$) of MCE/Tilmicosin (Pre-incubation) against PRRSV was determined. (D) The $EC_{50}$ of MCE/Tilmicosin (Post-incubation) against PRRSV was determined. (E) The $EC_{50}$ of MCE/Tilmicosin (Co-incubation) against PRRSV was determined. The data represent the mean values from three independent experiments. * P<0.05; ** P<0.01; *** P<0.001.

To investigate the impact of MCE on PRRSV replication, cells were exposed to concentrations of MCE ranging from 0.19 to 6.25mg/mL and then infected with PRRSV. The PRRSV's ORF7 mRNA and N protein levels were monitored by qPCR, western blot, and IFA. The results showed that the PRRSV ORF7 copies were significantly reduced in the MCE-treated group (pre-, co-, post-incubation) compared to the PRRSV-infection group (Fig. 2A). Similarly, the N protein expression and viral titer levels were significantly reduced (Fig. 2B-E). These results indicate that MCE exhibits dose-dependent anti-PRRSV activity.

Furthermore, the effects of MCE on viral adsorption and internalization were investigated. The results showed that, compared with the control group (adsorption stage: $1.75 \pm 0.09 \times 10^6$ copies; internalization stage: $9.77 \pm 0.50 \times 10^5$), the PRRSV ORF7 gene in the MCE-treated (6.25 mg/mL) group (adsorption stage: $1.02 \pm 0.02 \times 10^6$; internalization stage: $5.26 \pm 0.39 \times 10^5$) was significantly reduced ($P<0.05$; Fig. 2F). Compared with the PRRSV group, the green fluorescence of the MCE treatment group was significantly reduced in Marc-145 and PAM cells (Fig. 3). To summarize, MCE demonstrated notable anti-PRRSV effects.

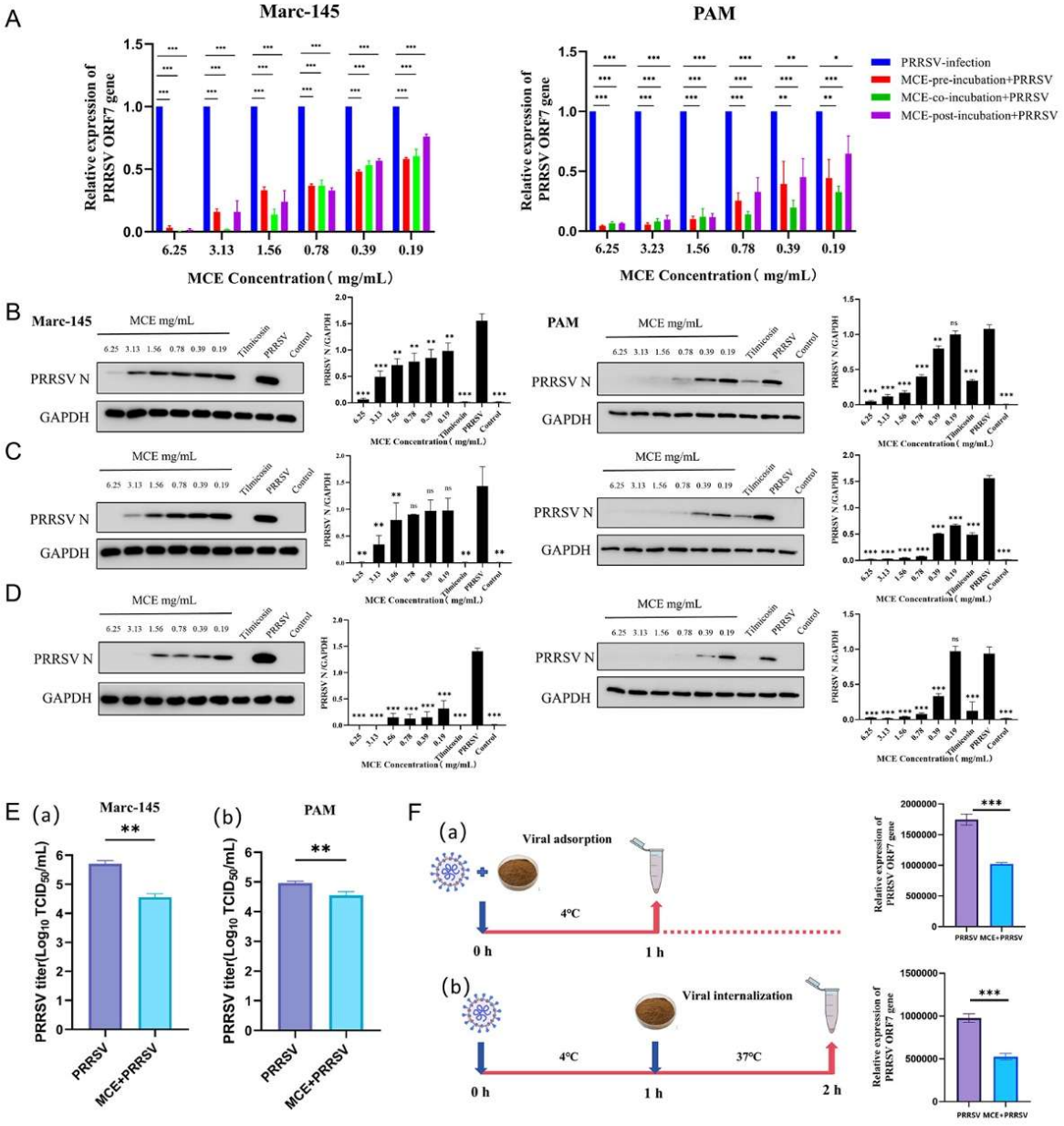


**Fig. 2:** MCE inhibits PRRSV proliferation in a dose-dependent manner and suppresses viral adsorption and internalization. (A) Changes in the ORF7 gene of PRRSV-infected Marc-145/PAM cells following MCE treatment. (B-D) Changes in N protein levels of PRRSV-infected Marc-145/PAM cells following MCE treatment. B: Pre-incubation; C: Post-incubation; D: Co-incubation. (E) Effect of MCE co-incubation treatment on PRRSV titer in Marc-145 cells (a) and PAM cells (b). Viral titers were determined by $TCID_{50}$ assay (calculated using the Reed-Muench method) and are expressed as Log10 $TCID_{50}$/mL. (F) The effect of MCE on the adsorption and internalization stages of PRRSV. a: adsorption stage; b: internalization stage. 10mM Tilmicosin was used as a positive control. The data represent the mean values from three independent experiments. * $P<0.05$; ** $P<0.01$; *** $P<0.001$.

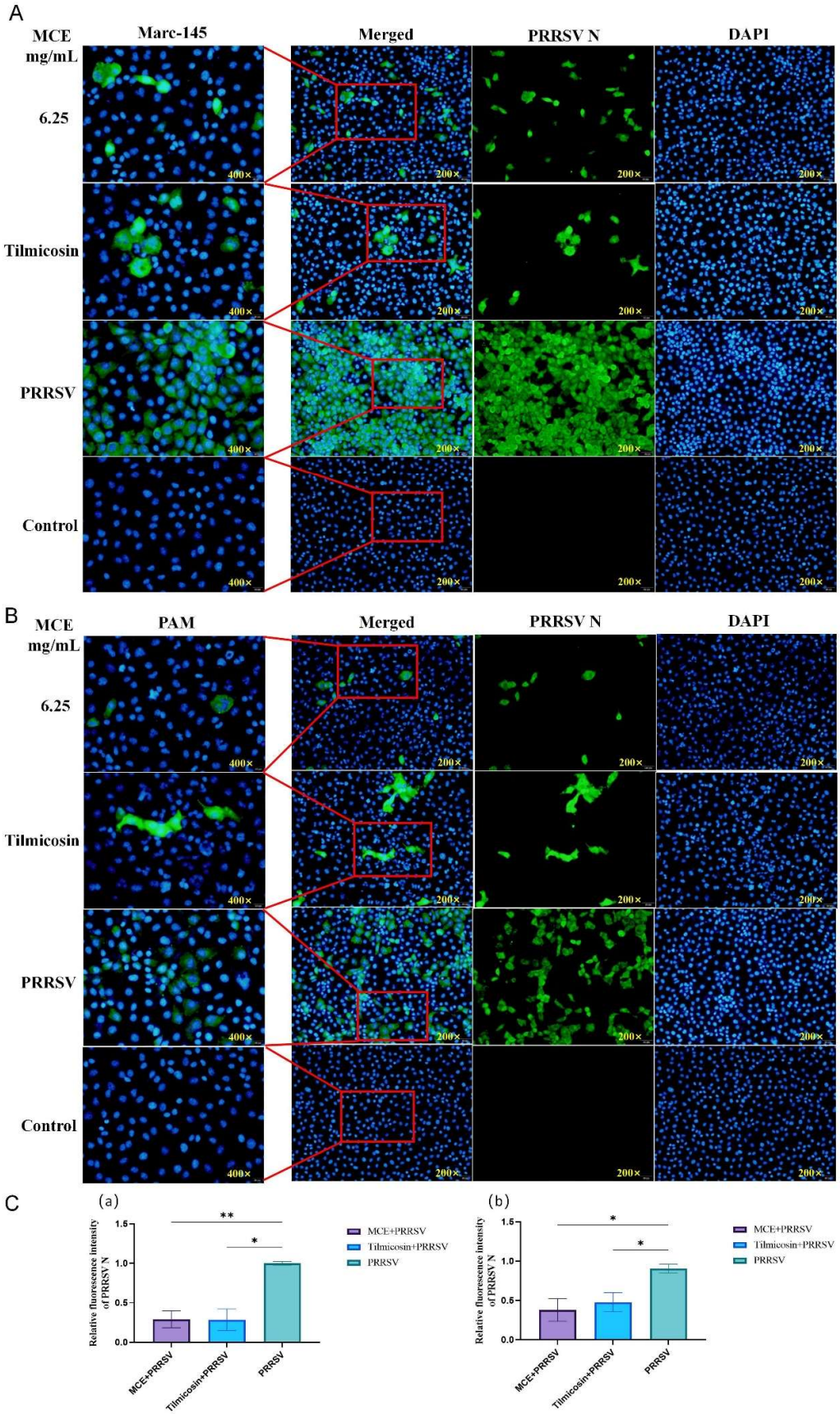


**Fig. 3:** Fluorescence changes of PRRSV N protein in Marc-145 cells treated with different concentrations of MCE. (A) Marc-145 cells. (B) PAM cells. 10 mM Tilmicosin was used as a positive control. (C) Relative fluorescence intensity of PRRSV N in Marc-145 cells (a) and PAM cells (b). The data represent the mean values from three independent experiments. * P<0.05; ** P<0.01; *** P<0.001.

**Prediction of MCE anti-PRRSV targets based on network pharmacology and molecular docking:** A total of seven MCE active chemical components were obtained using the HERB online database, including *allocryptopine*, *bocconoline*, *chelerythrine*, *ethoxychelerythrine*, *ethoxysanguinarine*, *oxysanguinarine*, and *sanguinarine*. All these compounds satisfy Lipinski's rule of five and can be screened for future targets. Four hundred forty target genes were predicted for MCE, and 4,790 disease targets were predicted for PRRSV, resulting in 169 shared targets (Fig. 4A). The "drug-compound-target-disease" network consists of 178 nodes (7 active compound nodes, 169 target nodes, 1 MCE node, and 1 PRRS node) and 504 edges (Fig. 4B). The preliminary construction of monkey (*Chlorocebus sabaeus*)- and pig (*Sus scrofa*)-derived PPI network maps is commencing with the import of 169 targets into the String website. Since virus replication relies on host factors, choosing monkey and pig targets homologous to the cell model for molecular docking can better represent the compound's cellular activity and mechanisms. The PPI network was subjected to topological analysis, and the data from *Chlorocebus sabaeus* and *Sus scrofa* were screened to obtain 25 core targets, respectively (Fig. 4C). The top 5 targets of the Degree score were calculated using Cytoscape 3.6.1, and their intersections were used to obtain the final 3 drug components-disease common core targets of monkey and pig origin (Fig. 4C). TP53, ESR1, and EGFR are identified as the main targets for addressing PRRSV by MCE (Fig. 4D). Notably, EGFR showed the most significant changes among the three targets and was deemed the most critical for further study (Fig. 4D).

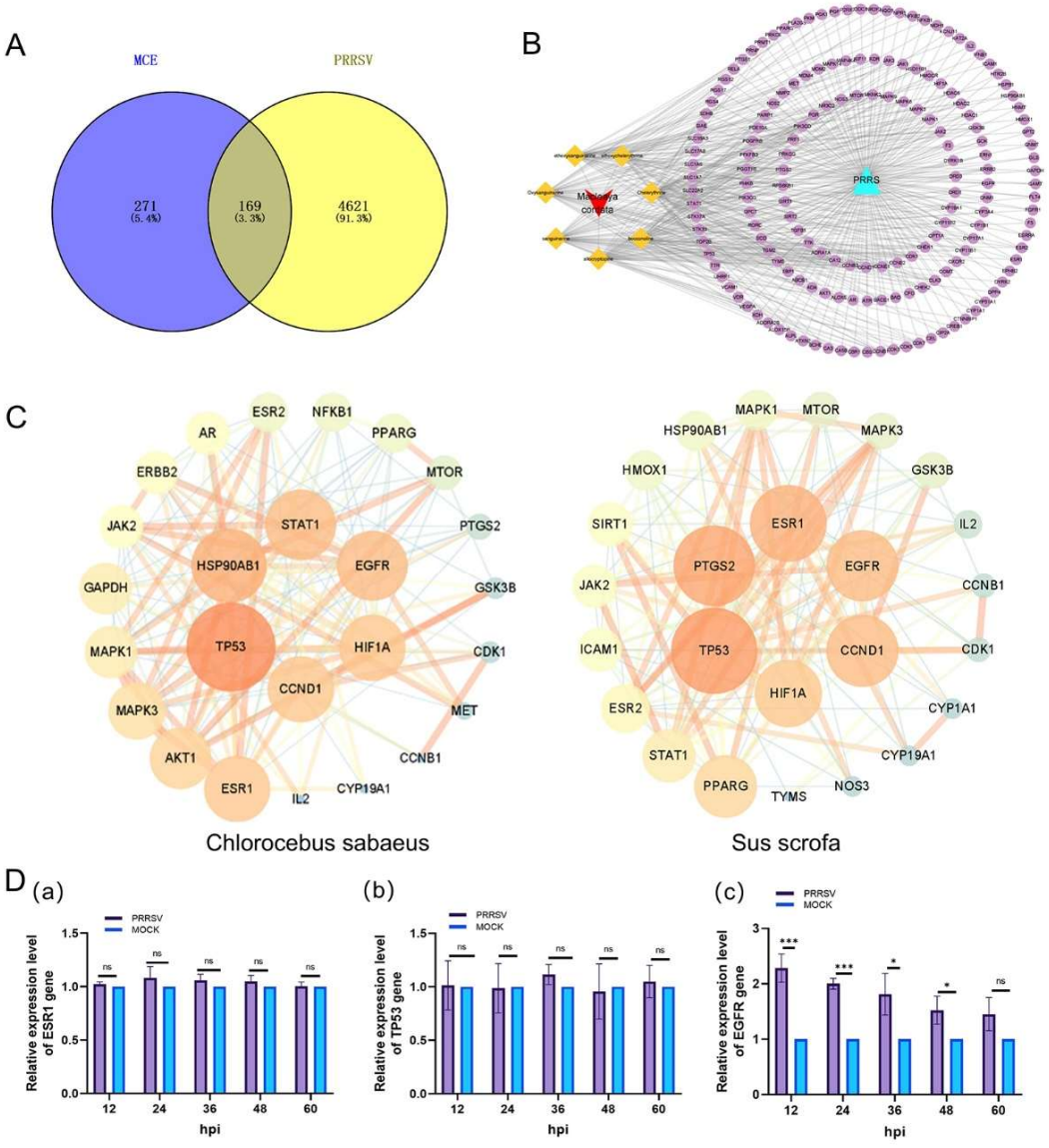


**Fig. 4:** Screening for potential PRRSV targets in MCE. (A) Venn diagram of MCE active ingredient target-PRRS disease target. (B) "Drug-Compound-Target-Disease" interaction network. The orange diamond represents the active compound, and the purple circle represents the intersection of MCE active compounds and PRRS target genes. (C) Chlorocebus sabaeus and Sus scrofa origin "component-disease" networks. (D) Effects of PRRSV infection on the expression levels of EGFR, TP53, and ESR1 genes. The data represent the mean values from three independent experiments. * P<0.05; ** P<0.01; *** P<0.001.

Molecular docking and visualization were conducted for seven active small-molecule compounds from the MCE that target EGFR. The docking results indicated that the EGFR protein could bind to 5 active compounds, including *ethoxychelerythrine*, *allophanine*, *oxyhaemonine*, *haemonine*, and *chelerythrine* (Fig. 5A-B, Table 3). This result suggests that the EGFR might be involved in inhibiting PRRSV infection by binding to these compounds.

**Table 3:** Molecular docking results

| No. | Molecular | Score |
|---|---|---|
| 1 | *Ethoxychelerythrine* | -5.328 |
| 2 | *Oxysanguinarine* | -2.945 |
| 3 | *Sanguinarine* | -2.289 |
| 4 | *Allocryptopine* | -4.628 |
| 5 | *Chelerythrine* | -4.274 |
| 6 | *Sanguinarine* | -2.596 |
| 7 | *Chelerythrine* | -1.715 |

This table presents binding energy or affinity data for each binding pocket of the target protein to characterize potential interactions with the compound.

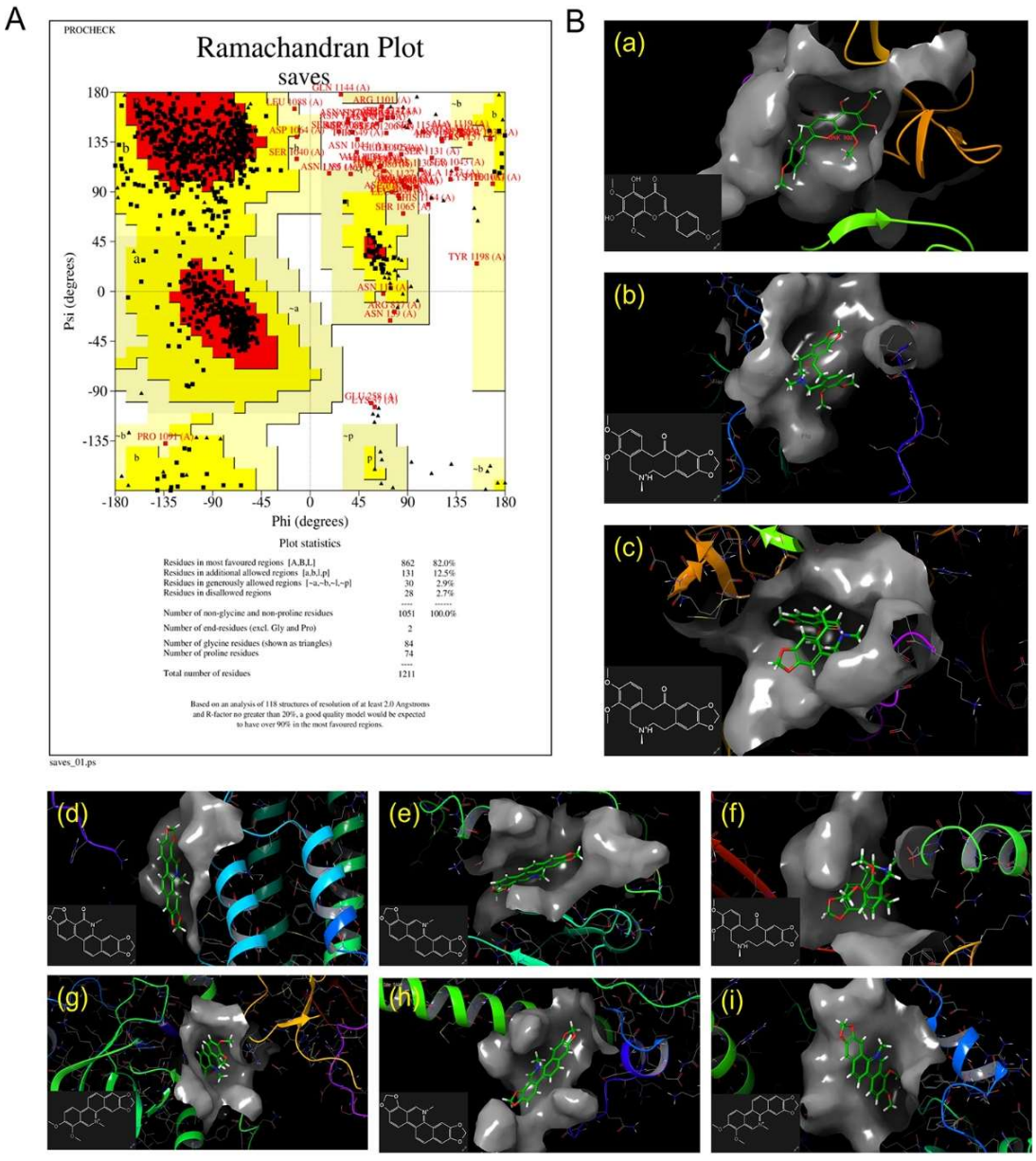


**Fig. 5:** Verification of the binding between EGFR and PRRSV targets (A) Ramachandran diagram of the EGFR protein model. (B) Visualization of 9 docking results of EGFR.

**MCE-targeted binding of EGFR inhibits PRRSV replication:** After knockdown of EGFR by siRNA and inoculation of PRRSV, changes in PRRSV ORF7 gene expression were detected by qRT-PCR, while changes in the expression of PRRSV N protein, EGFR protein, and p-EGFR protein were detected by Western blot. The results showed that knockdown of EGFR significantly downregulated the EGFR mRNA levels (Fig. 6A) and protein levels of EGFR and phosphorylated EGFR (p-EGFR) (Fig. 6B). Additionally, EGFR knockdown significantly inhibited PRRSV replication, as evidenced by reduced ORF7 mRNA (Fig. 6C) and N protein levels (Fig. 6D).

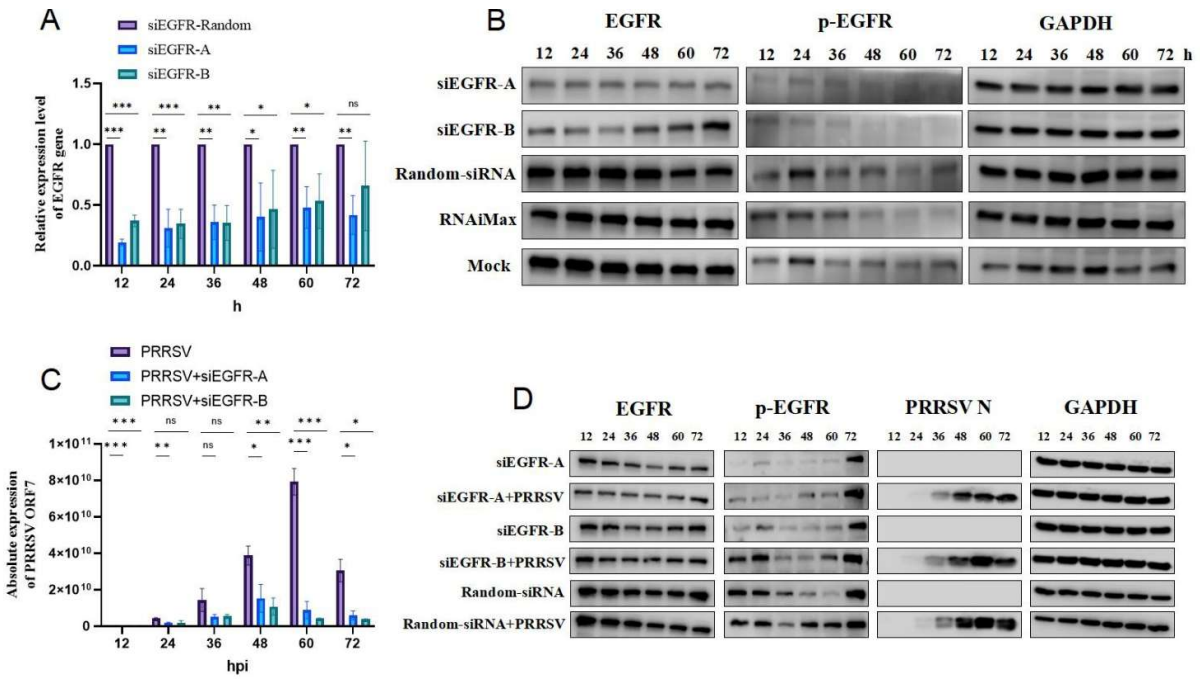


**Fig. 6:** Knocking down EGFR inhibits PRRSV replication. (A) Effect of siRNA knockdown on EGFR mRNA level. (B) Effect of siRNA knockdown on EGFR protein level. (C) Effect of EGFR knockdown on PRRSV ORF7 mRNA level. (D) Effect of EGFR knockdown on PRRSV N protein level. The data represent the mean values from three independent experiments. * P<0.05; ** P<0.01; *** P<0.001.

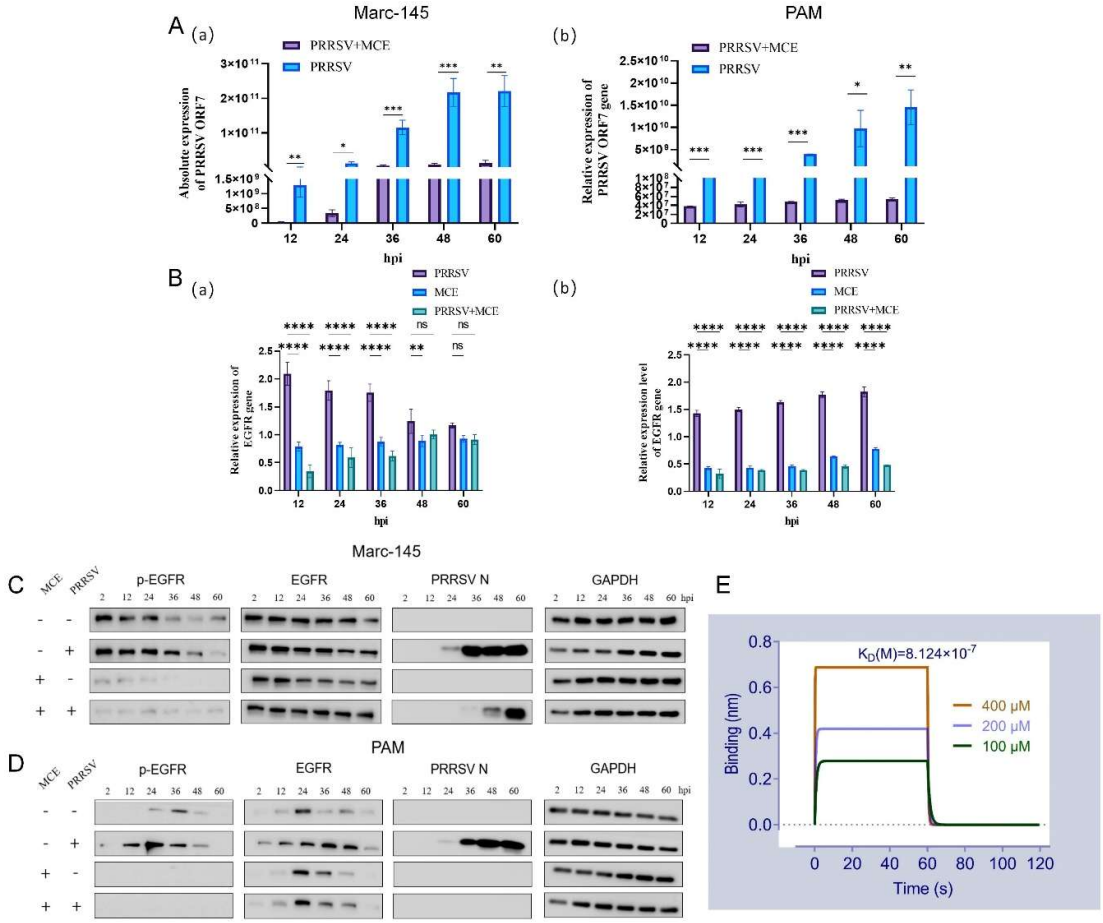


**Fig. 7:** MCE targets EGFR to inhibit PRRSV proliferation. (A) Absolute expression of PRRSV ORF7 gene in Marc-145 cells (a) and PAM cells (b) treated with MCE. (B) Relative expression of the EGFR gene in Marc-145 cells (a) and PAM cells (b) treated with MCE. (C) Expression of N proteins in Marc-145 cells treated with MCE and PRRSV. (D) Expression of N proteins in PAM cells treated with MCE and PRRSV. (E) Determination of binding affinity of different concentrations of MCE to EGFR. The data represent the mean values from three independent experiments. * P<0.05; ** P<0.01; *** P<0.001.

To determine whether EGFR is a target for MCE against PRRSV, Marc-145 cells were treated with 6.25 mg/mL MCE and subsequently inoculated with PRRSV. The levels of ORF7 mRNA, N protein of PRRSV, EGFR, and p-EGFR expression were then detected. The results showed that the expression level of the PRRSV ORF7 gene was significantly reduced in the MCE-treated group at all five time points (12, 24, 36, 48, and 60 hpi) compared with the PRRSV-infection group ($P<0.05$; Fig. 7A), as well as the expression level of the EGFR gene ($P<0.05$; Fig. 7B). Knockdown of EGFR significantly downregulated PRRSV N protein expression levels, along with a significant decrease in EGFR and p-EGFR protein expression ($P<0.05$; Fig. 7C-D). The BLI assay results demonstrated that, as the concentration of MCE increases, the binding signal between MCE and EGFR also increases ($K_D(M)=8.124 \times 10^{-7}$, Fig. 7E), indicating that MCE can exert its effect by targeting EGFR. Taken together, MCE inhibits PRRSV proliferation by targeting the expression of EGFR and phosphorylation (Fig. 8).

## DISCUSSION

PRRS is one of the primary factors contributing to the porcine respiratory disease complex (PRDC), posing a significant threat to the global pig industry (Risser *et al.*, 2021). Due to the high variability and immune evasion characteristics of PRRSV, as well as the overuse of antibiotics in the pig farming system, the PRRS epidemic is severe and difficult to control. Therefore, developing antiviral drugs with low drug resistance and high efficiency is paramount.

It is reported that a variety of antiviral drugs targeting PRRSV have been screened and identified so far, including herbal extracts, chemical compounds, and nanobodies (Du *et al.*, 2017; Chen *et al.*, 2025). Herbal extracts are a type of traditional Chinese medicine. Compared with chemical drugs, traditional Chinese medicine has the advantages of low drug resistance, low cost, low toxicity, few side effects, and diverse administration methods (Li *et al.*, 2004; Yuan *et al.*, 2016), and it plays an important role in antiviral treatment. Different traditional Chinese medicines exert antiviral effects at different stages of PRRSV infection and proliferation. Some traditional Chinese medicines can inhibit PRRSV by influencing specific steps in the attachment, internalization, replication, and release of PRRSV, while others can regulate the immune response of the body and enhance antiviral ability (Bello-Onaghise *et al.*, 2020; Zhang *et al.*, 2022). In this study, molecular docking, network pharmacology, and biofilm interference techniques were used to analyze and verify that MCE can target and inhibit PRRSV infection through EGFR, thereby providing new insights and theoretical support for the development of antiviral drugs for PRRSV.

MCE is an extract of traditional Chinese medicine and has been proven to play a significant role in inhibiting microbial growth, preventing fungal infections, and exhibiting antiviral effects (Chaturvedi *et al.*, 1997; Ming *et al.*, 2011; Wang *et al.*, 2012). Both *in vivo* and *in vitro* experiments have found that MCE plays an important role. Existing studies have shown that the addition of MCE can improve growth performance and enhance the immune response and antiviral ability of newborn piglets (Han *et al.*, 2024). During *in vitro* experiments, relevant studies have found that the main component of MCE, sanguinarine (SG), can act on the internalization and replication stages of the PRRSV life cycle and has an anti-PRRSV effect (Ke *et al*., 2023). However, the mechanism by which MCE interacts with PRRSV to exert its anti-PRRSV effect remains unclear. In this study, we found that MCE could inhibit the replication of PRRSV in a dose-dependent manner, which is consistent with previous reports (Ke *et al*., 2023), further demonstrating that MCE can be used as an effective drug against PRRSV. Research indicates that while Sanguinarine alone has promising antiviral properties by blocking early virus entry, its narrow therapeutic window limits clinical use. In contrast, the total extract, containing multiple active components like flavonoids and phenolic acids, offers enhanced antiviral effects through multi-target synergy and reduces toxicity, thus widening the therapeutic window. Additionally, the simple and cost-effective preparation process supports its inclusion in antiviral strategies for clinical trials.

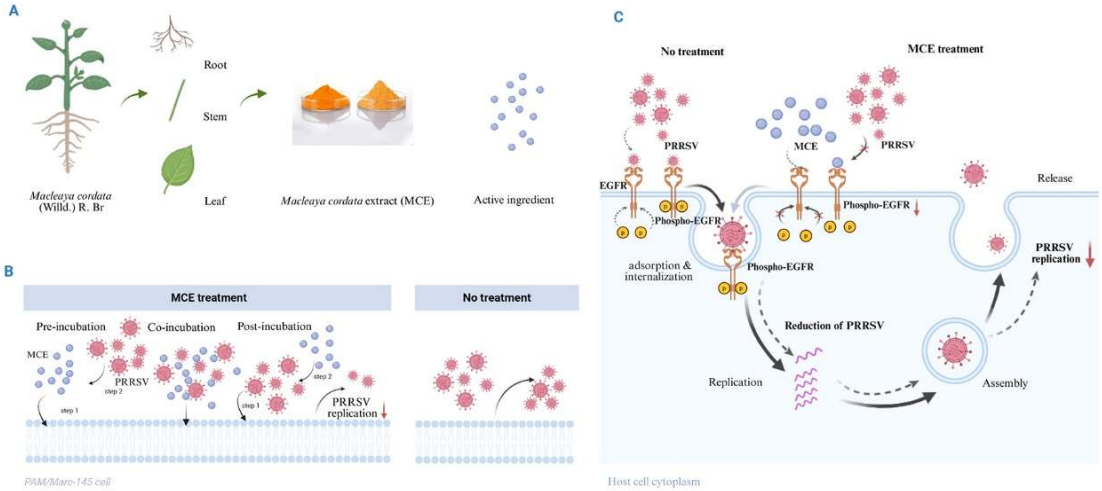


**Fig. 8:** Schematic diagram of the mechanism by which *Macleaya cordata* extract targets EGFR to antagonize PRRSV infection. (A) Source and bioactive components of MCE. (B) MCE exerts anti-PRRSV effects through three treatment modalities. (C) Antagonism of PRRSV infection by *Macleaya cordata* extract targeting EGFR.

To further investigate how MCE acts against PRRSV, we have designed three modes: preventive, therapeutic, and direct. The experimental results show that all three action modes can inhibit PRRSV, among which MCE has the strongest inhibitory effect in the direct-action mode. Moreover, the antiviral effect of MCE treatment is mainly achieved by inhibiting the ability of the virus to adsorb and to invade host cells. This study shows that MCE has strong anti-PRRSV effects in vitro. Although MCE is known to boost piglets' immune systems, its antiviral mechanisms in living organisms need more research (Han *et al*., 2024). Future studies will use *in vivo* models to assess its potential for clinical use.

Different antiviral traditional Chinese medicines have different antiviral mechanisms against various viral infections. For instance, the artemisinin-derived antimalarial drug artesunate, extracted from Artemisia annua, can inhibit the replication of PRRSV by regulating the AMPK and Nrf2/HO-1 signaling pathways (Long *et al.*, 2022). The active compound Sanggenon C, extracted from mulberry bark, has been confirmed to inhibit PRRSV replication by regulating the TRAF2/NF-κB signaling pathway(Liu *et al.*, 2023). This study utilized network pharmacology and molecular docking techniques to predict the potential targets of MCE against PRRSV, and screened and identified TP53, ESR1, and EGFR as the core potential targets. Among these, it is worth noting that EGFR (a tyrosine kinase receptor of the ErbB family) has been identified as the core target that plays a key role. EGFR activates tyrosine kinase activity by binding to ligands such as epidermal growth factor (EGF), thereby influencing multiple intracellular signaling pathways and regulating several processes, including cell proliferation, differentiation, migration, and survival (Wells, 1999). Previous studies have shown that EGFR is a key co-receptor for the invasion of PRRSV, hepatitis C virus, influenza A virus, and human cytomegalovirus (Eierhoff *et al.*, 2010).

Furthermore, studies have found that the surface glycoproteins (HN and F proteins) of bovine parainfluenza virus 3 (BPIV3) and the surface S protein of transmissible gastroenteritis virus (TGEV) can bind to EGFR on the surface of host cells (Wang *et al.*, 2016), which is conducive to viral infection. In the early stage of Japanese encephalitis virus (JEV) infection, the phosphorylation of EGFR can be activated (Noh and Shin, 2023). Studies have shown that syndecan-4 can interact with EGFR on the surface of Marc-145 cells during PRRSV infection and mediate the endocytosis of PRRSV by activating EGFR (Li *et al.*, 2022). Our earlier findings showed that MCE can prevent PRRSV adsorption, possibly by altering EGFR conformation or blocking its binding sites, or by changing the virus structure through redox reactions. BLI experiments confirmed that MCE targets EGFR on host cells in a dose-dependent manner, hindering PRRSV's initial adsorption. Research on a single PRRSV strain may not represent other prevalent strains like NADC30-like, and the antiviral activity of MCE may differ across genotypes.

**Conclusions:** Understanding the mechanism by which traditional Chinese medicine exerts antiviral effects by regulating the relevant signaling pathways of host cells is both a research challenge and a hot topic in the future development of new antiviral drugs. Our experimental results indicate that EGFR serves as a potential target for MCE's anti-PRRSV activity. MCE inhibits EGFR phosphorylation, thereby indirectly countering PRRSV infection. Our research further demonstrates the great potential of MCE in the prevention and control of PRRS, broadens perspectives for exploring the antiviral mechanisms of traditional Chinese medicine, and highlights the value of repurposing old drugs.

**Acknowledgements:** This work is supported by Yunnan Provincial Innovation Team of Key Technologies for Prevention and Control of Important Livestock and Poultry Diseases [grant number 202405AS350004], National Natural Science Foundation of China (grant number 32260877), Yunnan Province Joint Special Project on Agricultural Basic Research-Key Project (grant number 202301BD070001-140) and The Yunnan Province Special Project for Building a Science and Technology Innovation Center for South and Southeast Asia -Yunnan Province International Joint Research and Development Center for Veterinary Pharmaceuticals [grant number 202403AP140012].

**Authors contribution:** Gefen Yin and ZhenLei Zhou conceived and designed the study. Yongneng Li, Jiaxing Sun, and Shanshan Qi conducted the investigation. Xinxian Wang, Wenjuan Su, Qian Li, and Yongmei Li were responsible for data curation. Shanshan Qi and Junlong Bi provided project administration. Yongneng Li drafted the original manuscript. ZhenLei Zhou, along with all other authors, participated in reviewing and editing the manuscript, and all have read and approved the final version.

**Availability of data and materials:** All the data contained within this manuscript.

**Declaration of interest:** The authors declare that they have no competing interests.

## REFERENCES

Albina E, 1997. Epidemiology of porcine reproductive and respiratory syndrome (PRRS): an overview. Veterinary Microbiology 55:309-316.

Bello-Onaghise G, Wang G, Han X, *et al.*, 2020. Antiviral strategies of Chinese Herbal Medicine against PRRSV infection. Frontiers in Microbiology 11:1756.

Bi J, Zhao Q, Zhu L, *et al.*, 2018. RACK1 is indispensable for porcine reproductive and respiratory syndrome virus replication and NF-κB activation in Marc-145 cells. Scientific Reports 8:2985.

Chang H, Gao X, Wu Y, *et al.*, 2024. Genomic and pathogenicity analysis of two novel highly pathogenic recombinant NADC30-like PRRSV strains in China, in 2023. Microbiology Spectrum 12:e0036824.

Chaturvedi M M, Kumar A, Darnay B G, *et al.*, 1997. Sanguinarine (pseudochelerythrine) is a potent inhibitor of NF-kappaB activation, IkappaBalpha phosphorylation, and degradation. The Journal of Biological Chemistry 272:30129-30134.

Chen H, Weng C, Huang X, *et al.*, 2025. Integrated PRRSV prevention and control strategy based on the One Health concept: across the boundaries of virology, ecology and public health. Frontiers in Microbiology 16:1718572.

Chen K and Yu B, 1999. Certain progress of clinical research on Chinese integrative medicine. Chinese Medical Journal 112:934-937.

Chen R, Liu B, Zhang X, *et al.*, 2022. A porcine reproductive and respiratory syndrome virus (PRRSV)-specific IgM as a novel adjuvant

for an inactivated PRRSV vaccine improves protection efficiency and enhances cell-mediated immunity against heterologous PRRSV challenge. Veterinary Research 53:65.

Collins JE, Benfield DA, Christianson WT, *et al.*, 1992. Isolation of swine infertility and respiratory syndrome virus (isolate ATCC VR-2332) in North America and experimental reproduction of the disease in gnotobiotic pigs. The Journal of Veterinary Diagnostic Investigation 4:117-126.

Du T, Nan Y, Xiao S, *et al.*, 2017. Antiviral Strategies against PRRSV Infection. Trends in Microbiology 25:968-979.

Eierhoff T, Hrincius ER, Rescher U, *et al.*, 2010. The epidermal growth factor receptor (EGFR) promotes uptake of influenza A viruses (IAV) into host cells. PLoS Pathogens 6:e1001099.

Forsberg R, Storgaard T, Nielsen HS, *et al.*, 2002. The genetic diversity of European type PRRSV is similar to that of the North American type but is geographically skewed within Europe. Virology 299:38-47.

Guo Z, Chen XX, Li R, *et al.*, 2018. The prevalent status and genetic diversity of porcine reproductive and respiratory syndrome virus in China: a molecular epidemiological perspective. Virology Journal 15:2.

Guo BQ, Chen ZS, Liu WX, *et al.*, 1996. Isolation of PRRSV from Suspected PRRS Aborted Fetuses. Chinese Journal of Animal and Poultry Infectious Diseases: 3-7. (in Chinese)

Han D, Yang H, Li J, *et al.*, 2024. Macleaya cordata extract improves growth performance, immune responses and anti-inflammatory capacity in neonatal piglets. Veterinary Microbiology 293:110090.

Holmes J A, Rutledge S M, Chung R T, 2019. Direct-acting antiviral treatment for hepatitis C. The Lancet 393:1392-1394.

Jiao S, Zhang J, Wang J, *et al.*, 2024. Whole-genome analysis of the recombination and evolution of newly identified NADC30-like porcine reproductive and respiratory syndrome virus strains circulated in Gansu province of China in 2023. Frontiers in Veterinary Science 11:1372032.

Ke Q, Duan K, Cheng Y, *et al.*, 2023. Sanguinarine Exhibits Antiviral Activity against Porcine Reproductive and Respiratory Syndrome Virus via Multisite Inhibition Mechanisms. Viruses 15.

Keffaber KK, 1989. Reproductive failure of unknown etiology. American Association of Swine Practitioners Newsletter 1: 1-10.

Kosina P, Gregorova J, Gruz J, *et al.*, 2010. Phytochemical and antimicrobial characterization of Macleaya cordata herb. Fitoterapia 81:1006-1012.

Kuwahara H, Nunoya T, Tajima M, *et al.*, 1994. An outbreak of porcine reproductive and respiratory syndrome in Japan. The Journal of Veterinary Medical Science 56:901-909.

Li C, Zhuang J, Wang J, *et al.*, 2016. Outbreak Investigation of NADC30-Like PRRSV in South-East China. Transboundary and Emerging Diseases 63:474-479.

Li R, Qiao S, Zhang G, 2022. Reappraising host cellular factors involved in attachment and entry to develop antiviral strategies against porcine reproductive and respiratory syndrome virus. Frontiers in Microbiology 13:975610.

Li WL, Zheng HC, Bukuru J, *et al.*, 2004. Natural medicines used in the traditional Chinese medical system for therapy of diabetes mellitus. Journal of Ethnopharmacology 92:1-21.

Lin L, Liu YC, Huang JL, *et al.*, 2018. Medicinal plants of the genus Macleaya (Macleaya cordata, Macleaya microcarpa): A review of their phytochemistry, pharmacology, and toxicology. Phytotherapy Research 32:19-48.

Lin WH, Kaewprom K, Wang SY, *et al.*, 2020. Outbreak of Porcine Reproductive and Respiratory Syndrome Virus 1 in Taiwan. Viruses 12.

Liu X, Bi J, Zhao Q, *et al.*, 2019. Overexpression of RACK1 enhanced the replication of porcine reproductive and respiratory syndrome virus in Marc-145 cells and promoted the NF-κB activation via upregulating the expression and phosphorylation of TRAF2. Gene 709:75-83.

Liu X, Zhu Y, Wang D, *et al.*, 2023. The natural compound Sanggenon C inhibits PRRSV infection by regulating the TRAF2/NF-κB signalling pathway. Veterinary Research 54:114.

Long F, Zhang M, Yang X, *et al.*, 2022. The antimalaria drug artesunate inhibits porcine reproductive and respiratory syndrome virus replication by activating AMPK and Nrf2/HO-1 Signaling Pathways. Journal of Virology 96:e0148721.

Lunney JK, Fang Y, Ladinig A, *et al.*, 2016. Porcine Reproductive and Respiratory Syndrome Virus (PRRSV): pathogenesis and interaction with the immune system. Annual Review of Animal Biosciences 4:129-154.

Manyi-Loh C, Mamphweli S, Meyer E, *et al.*, 2018. Antibiotic use in agriculture and its consequential resistance in environmental sources: potential public health implications. Molecules 23(4): 795.

Ming Z, Li GY, Zeng JG, *et al.* 2011. Evaluation of molluscicidal activities of benzo(c)phenanthridine alkaloids from Macleaya cordata (Willd) R. Br. on snail hosts of Schistosoma japonicum. Journal of Medicinal Plants Research 5(4): 521-526.

Noh SS and Shin HJ, 2023. Role of Virus-Induced EGFR Trafficking in Proviral Functions. Biomolecules 13(12): 1766.

Risser J, Ackerman M, Evelsizer R, *et al.*, 2021. Porcine reproductive and respiratory syndrome virus genetic variability a management and diagnostic dilemma. Virology Journal 18:206.

Shi YB, Liu L, Shao W, *et al.*, 2015. Microcalorimetry studies of the antimicrobial actions of Aconitum alkaloids. Journal of Zhejiang University Science B 16:690-695.

Tian K, Yu X, Zhao T, *et al.*, 2007. Emergence of fatal PRRSV variants: unparalleled outbreaks of atypical PRRS in China and molecular dissection of the unique hallmark. PLoS One 2:e526.

VanderBurgt JT, Harper O, Garnham CP, *et al.*, 2023. Plant production of a virus-like particle-based vaccine candidate against porcine reproductive and respiratory syndrome. Frontiers in Plant Science 14:1044675.

Wang HM, Liu YG, Tang YD, *et al.*, 2018. A natural recombinant PRRSV between HP-PRRSV JXA1-like and NADC30-like strains. Transboundary and Emerging Diseases 65:1078-1086.

Wang K, Luo C, Liu H, *et al.*, 2012. Nematicidal activity of the alkaloids from Macleaya cordata against certain nematodes. African Journal of Agricultural Research 7:5925-5929.

Wang R, Wang X, Ni B, *et al.*, 2016. Syndecan-4, a PRRSV attachment factor, mediates PRRSV entry through its interaction with EGFR. Biochemical and Biophysical Research Communications 475:230-237.

Wang X, Bi J, Yang Y, *et al.*, 2023. RACK1 promotes porcine reproductive and respiratory syndrome virus infection in Marc-145 cells through ERK1/2 activation. Virology 588:109886.

Wells A, 1999. EGF receptor. The International Journal of Biochemistry & Cell Biology 31:637-643.

Wensvoort G, de Kluyver EP, Pol JM, *et al.*, 1992. Lelystad virus, the cause of porcine epidemic abortion and respiratory syndrome: a review of mystery swine disease research at Lelystad. Veterinary Microbiology 33:185-193.

Wensvoort G, Terpstra C, Pol JM, *et al.*, 1991. Mystery swine disease in The Netherlands: the isolation of Lelystad virus. The Veterinary Quarterly 13:121-130.

Xu H, Li C, Li W, *et al.*, 2022. Novel characteristics of Chinese NADC34-like PRRSV during 2020-2021. Transboundary and Emerging Diseases 69:e3215-e3224.

Yang HC, Guan SH, Yin XM, *et al.*, 1997. Isolation and preliminary identification of Porcine Reproductive and Respiratory Syndrome Virus. Chinese Journal of Veterinary Medicine: 9-10. (in Chinese)

Yuan H, Ma Q, Ye L, *et al.*, 2016. The traditional medicine and modern medicine from natural products. Molecules 21(5): 559.

Zhang HL, Zhang WL, Xiang LR, *et al.*, 2018. Emergence of novel porcine reproductive and respiratory syndrome viruses (ORF5 RFLP 1-7-4 viruses) in China. Veterinary Microbiology 222:105-108.

Zhang X, Chen S, Li X, *et al.*, 2022. Flavonoids as potential antiviral agents for porcine viruses. Pharmaceutics 14(9): 1793.

Zhao HZ, Wang FX, Han XY, *et al.*, 2022. Recent advances in the study of NADC34-like porcine reproductive and respiratory syndrome virus in China. Frontiers in Microbiology 13:950402.

Zhou L, Wang Z, Ding Y, *et al.*, 2015. NADC30-like strain of Porcine Reproductive and Respiratory Syndrome Virus, China. Emerging Infectious Diseases 21:2256-2257.